Aero-Sol−Gel Synthesis of Nanoporous Iron-Oxide Particles: A Potential Oxidizer for Nanoenergetic Materials

Anand Prakash, Alon V. McCormick, and Michael R. Zachariah*

Departments of Mechanical and Chemical Engineering, University of Minnesota, Minneapolis, Minnesota 55455

Received August 8, 2003. Revised Manuscript Received January 22, 2004

Interest in developing an oxidizer matrix for reaction with nano-aluminum for energy-intensive applications involving explosives and propellants have led to the development of an aerosol-based sol−gel method (Aero-sol−gel) for preparing nanoporous iron-oxide nanoparticles with high internal surface area. We have employed sol−gel reactions in the aerosol phase using an iron(III) salt with an epoxide in a volatile solvent (ethanol), to generate nanoporous oxidizer nanoparticles. Porosity of the particles results from the nature of the sol−gel chemistry implemented. Energy-dispersive spectrometry (EDS) results indicate that the aerosol-based chemistry is qualitatively similar to that occurring in bulk sol−gel synthesis. The oxidizer particles obtained from the aero-sol−gel experiment are in the 100−250-nm size range as evidenced by SEM and differential mobility analysis (DMA). Porosity of particles is observed qualitatively in the TEM micrographs and quantitatively determined with BET surface area measurements which indicate that these particles have total surface area that is enhanced by a factor of 200 over the geometric surface area. The aero-sol−gel derived iron oxide has also been mixed with nano-aluminum and preliminary ignition tests have been performed to show the effectiveness of the oxidizer particles.

I. Introduction

The class of materials used for applications involving propellants, explosives, and pyrotechnics are termed "energetic" materials. Typical preparation of such materials involves physical mixing of solid fuel and oxidizer powders. Mixing the fuel and oxidizer in stoichiometric proportions may maximize the energy density of the mixture, but the overall kinetics of the process still requires the two components to mix at the atomic scale in order for the reaction to take place. The larger the grain size of the particles (lower interfacial area between the oxidizer and fuel), the more the overall speed of the reaction will reflect the mass-transfer limitations. To achieve a chemical-kinetically controlled ignition, oxidizer materials with substantially larger surface area are required. Thus, a nanosized oxidizer and fuel material offer the potential (high surface area) for applications that involve rapid energy release.

There has been an increased research effort toward use of nano-aluminum in explosives.[1−4] A typical nanoenergetic material might be composed of nanoparticles of a fuel (e.g., aluminum) and an oxidizer (metal oxide), which react to liberate a large amount of energy according to the following thermite reaction.

$$Al + {}^{3}/_{2}MO \rightarrow {}^{1}/_{2}Al_2O_3 + {}^{3}/_{2}M + \Delta H$$

Table 1. Thermodynamics of Al Combustion in Different Oxidizers

reaction	adiabatic flame temp. [K]	ΔH (kJ/mol of Al)
$2Al + Fe_2O_3$	3198	−425
$2Al + 3CuO$	3794	−604
$2Al + MoO_3$	3812	−465

Examples of oxidizer particles include Fe_2O_3, MoO_3, and CuO. Thermodynamic characteristics of aluminum combustion[5] with the above three oxidizers are listed in Table 1 (adiabatic flame temperatures have been estimated from the NASA-GLENN chemical equilibrium program CEA).

In this paper we demonstrate a new approach to the synthesis of Fe_2O_3 via an aero-sol−gel based approach. In particular, the objectives were to generate a material with very high porosity, which might enable impregnation of organics which during combustion would generate a volatile product (gas).

Researchers at Lawrence Livermore Labs have successfully demonstrated the synthesis of porous solids for energetic material application through sol−gel methodologies,[6,7] which result in materials with high surface

* Corresponding author. E-mail: mrz@me.umn.edu.

(1) Ritter, H.; Braun, S. *Propellants, Explos., Pyrotech.* **2001**, *26*, 311.
(2) Ilyin, A.; Gromov, A.; An, V. *Propellants, Explos., Pyrotech.* **2002**, *27*, 361.
(3) Brousseau, P.; Anderson, C. J. *Propellants, Explos., Pyrotech.* **2002**, *27*, 300.
(4) Weiser, V.; Kelzenberg, S.; Eisenreich, N. *Propellants, Explos., Pyrotech.* **2001**, *26*, 284.
(5) Glassman, I. *Combustion*; Academic Press: New York, 1996.
(6) Gash, A. E.; Tillotson, T. M.; Satcher, J. H.; Hrubesh, L. W.; Simpson, R. L. *J. Non-Cryst. Solids* **2001**, *285*, 22.
(7) Tillotson, T. M.; Gash, A. E.; Simpson, R. L.; Hrubesh, L. W.; Satcher, J. H. *J. Non-Cryst. Solids* **2001**, *285*, 338.

10.1021/cm034740t CCC: $27.50
Published on Web 03/20/2004

area.[8] Our research aims at stabilizing aluminum nanoparticles by coating them with a material that not only protects them from spontaneous initiation but also acts as an oxidizer when ignition is initiated.[9] Indeed, we would want the oxidizer coating to provide high surface area for combustion of aluminum. While aerogels of these oxidizer materials have been synthesized in a batch process[10] (bulk), we believe that the particle morphology and ultimately quality control can be better manipulated in the gas phase. Hence, we propose an aerosol route to synthesis of such materials, and in the process we attempt to replicate batch chemistry in the aerosol phase.

Beaucage and co-workers have reported[11] what they term aero-sol−gel synthesis of nanostructured silica powders. In their approach they mix the precursors in the gas phase and the particles are formed via gas-phase polymerization/condensation. Their use of the term "aero-sol−gel" is meant to imply, as we understand it, as the use of sol−gel precursors as opposed to sol−gel chemistry. Our approach is to try to replicate the in batch experiments and truly do sol−gel chemistry within a small droplet.

In this paper we first describe a series of batch experiments to study the effects of temperature and solution concentration on gelation time. Since reaction time scales for bulk chemistries is on the order of hours and are therefore not amenable to aerosol synthesis, we discuss and demonstrate strategies for merging the two time scales in section II. Next, we describe the aerosol−gel method of atomizing a precursor solution, wherein the atomized droplets act as microreactors and host the sol−gel chemistry. The particle characteristics such as size, porosity, and composition are reported and an example of the reactive characteristics are shown.

II. Experimental Section

Batch Experiment. In the batch synthesis of Fe_2O_3 gel, hydrated iron(III) chloride ($FeCl_3 \cdot 6H_2O$) was used as the precursor and 1,2-epoxybutane was used as the complexing agent. Both the reagents were obtained from Aldrich. Absolute ethanol obtained from Aaper Alcohol was used as the solvent, and water was used as the gelation agent. $FeCl_3 \cdot 6H_2O$ (1.25 g) was added to 40 mL of absolute ethanol in a beaker and ultrasonicated for 20 min to obtain a clear yellow solution. To this mixture, 5 mL of epoxide and 1 mL of water were simultaneously added and the solution was stirred. This results in molar ratios of $[H_2O]/[FeCl_3 \cdot 6H_2O] = 12$ and [1,2-epoxybutane]/$[FeCl_3 \cdot 6H_2O] = 12.6$ for [Fe] = 0.1 M. The mixture was then allowed to sit until the solution formed a gel (time at which the solution could no longer flow). In the process of gel formation, the color of the solution gradually changes to reddish brown and the viscosity increases. Several sets of experiments with the same molar ratios of the reactants but with different [Fe] ([Fe] was varied by changing the amount of ethanol) were conducted and gelation time was observed as a function of molar concentration of the precursor salt. To study the role of temperature on the gelation kinetics, the reaction mixture was placed in a convection oven.

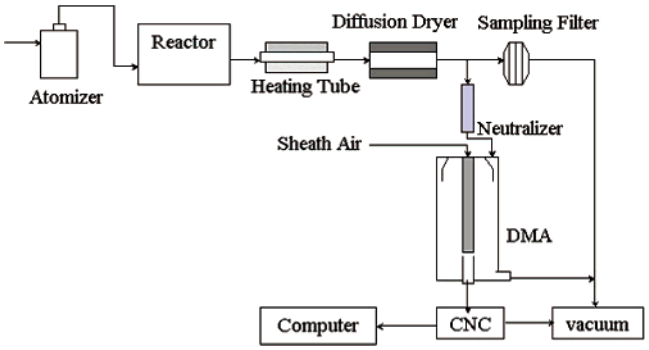

Figure 1. Schematic of the aerosol experimental system.

Aerosol Experiment. The aerosol reactor system is shown in Figure 1. Droplets of the precursor solution, prepared in the same fashion as in the batch experiments, were generated using dried/filtered air at a pressure of 35 psi in a collision-type atomizer. The geometric mean diameter[12] of the droplets were measured (~1 μm) with a laser aerosol spectrometer. The suspended aerosol droplets underwent drying, reaction, and gelation in a 45-L volume perfectly mixed-type reactor (PMR), which provides a residence time of about 15 min for a normal flow rate of 3 lpm. Following the PMR, the aerosol is passed through a heated flow tube (~80 °C) for approximately 3 s to vaporize any solvent that might still be present and subsequently passed through a carbon black diffusion dryer to absorb the solvent (ethanol) vapor, which might otherwise recondense on the particles. The particles were collected on a 0.6-μm DTTP membrane filter manufactured by Millipore and subsequently scraped off from the filter for offline analyses (microscopy, BET measurements, burn tests). Online size measurement of the particles was obtained using a home-built differential mobility analyzer (DMA) system and a TSI 3025 condensation nucleus counter.

III. Results and Discussion

Batch Experiments. The epoxide, when mixed with the precursor salt, acts as acid scavenger and apparently consumes protons from the hydrated Fe(III) species (Gash et al.[10]).

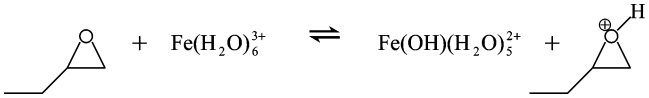

The Fe(III) complex on the right-hand side of the equation undergoes further hydrolysis and condensation to form Fe(III) oxide. Water is also added to the reactants as it was known that a certain minimum amount of water (3 equiv more than that predicted by stoichiometry, that is, $2Fe^{3+} + 3H_2O \rightarrow Fe_2O_3 + 6H^+$) is necessary for gelation to occur.[10] We observed, as presented in Figure 2, that the gelation kinetics is a strong positive function of precursor salt concentration, particularly so, at concentrations below about 0.1 M. However, below a concentration of 0.05 M in [Fe], the solution did not gel. The role of temperature on gelation kinetics is presented in Figure 3, which shows that higher temperatures favor faster gelation. The results indicate that below the boiling point of ethanol (78 °C) the gelation kinetics slows down considerably. This increase, however, may be attributable to two simultaneous effects. One is the usual increase in reaction rate

(8) Jarzebski, A. B.; Bialon, J. M.; Pajak, L. *Int. Conf. Eng. Educ.* **2001** (Aug), *7E1*, 13.
(9) Tillotson, T. M.; Hrubesh, L. W.; Simpson, R. L.; Lee, R. S.; Swansiger, R. W.; Simpson, L. R. *J. Non-Cryst. Solids* **1998**, *225*, 358.
(10) Gash, A. E.; Tillotson, T. M.; Satcher, J. H.; Poco, J. F.; Hrubesh, L. W.; Simpson, R. L. *Chem. Mater.* **2001**, *13*, 999.
(11) Beaucage, G.; Hyeon-Lee, J.; Kohls, D. J.; Pratsinis, S. E. *J. Nanopart. Res.* **1999**, *1*, 379.
(12) Kim, S. H.; Liu, B. Y. H.; Zachariah, M. R. *Chem. Mater.* **2002**, *14*, 2889.

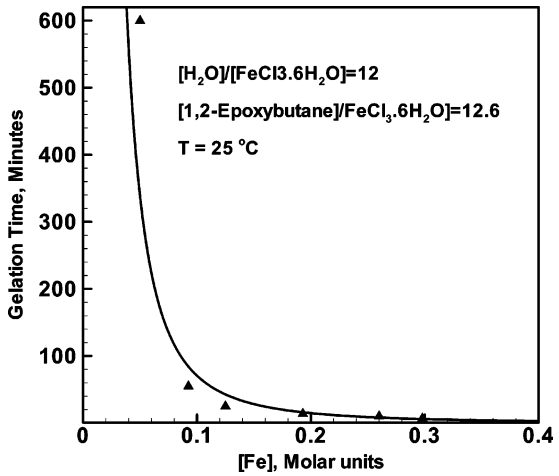

Figure 2. Variation of gelation time with precursor salt concentration at room temperature.

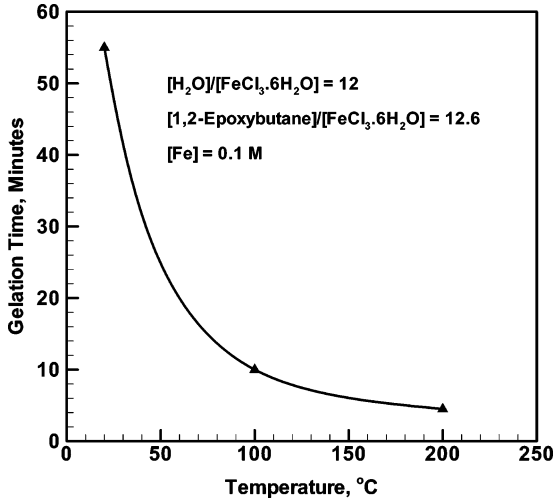

Figure 3. Gelation time dependence on temperature for a 0.1 M solution in [Fe].

due to higher temperatures. The other is that higher temperatures, particularly above the boiling point of ethanol, result in ethanol evaporation and correspondingly increases the iron concentration, resulting in a higher reaction rate. In the latter case when we conduct the experiment in the aerosol phase, we are effectively shrinking the reactor volume (i.e., droplet).

As shown in Figure 2, a 0.1 M [Fe] solution gelled after about an hour. Nevertheless, ^{13}C NMR experiments suggest that $FeCl_3$ decomposition (and complexation with the epoxide) occurs much faster and is essentially complete within 15 min, as evidenced by the time-resolved spectra shown in Figure 4 (peaks have not been assigned). The idea behind the time-resolved NMR experiment is to estimate the time scale over which chemical changes occur, rather than any mechanistic interpretation. The NMR result is consistent with the observation that the exothermic complexation reaction shows a temperature rise for the first 15 min, after which the reaction mixture begins to cool. Apparently, the gelation process, which occurs over a long time, occurs via physical aggregation of nanoparticles. The important inference from this observation is that we should be able to provide similar chemical species in the aerosol phase as those present in the bulk liquid phase, by allowing the bulk liquid to react on the order

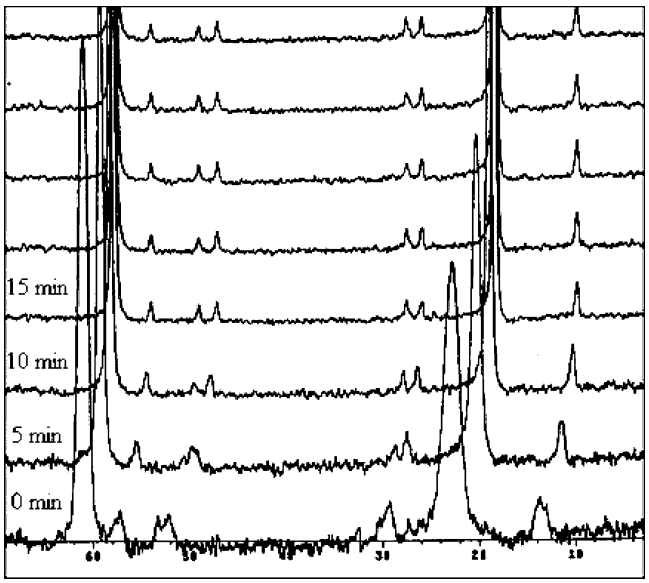

Figure 4. ^{13}C NMR spectra for a 0.1 [Fe] reaction mixture as a function of time.

of 15 min and then dispersing the liquid in aerosol, before gelation.

If no drying were to take place in the aerosol (i.e., if we were to provide a solvent and water saturated vapor phase), the gel time in the aerosol phase should be the same as in the bulk liquid. However, we have seen that the gel time is very sensitive to the precursor salt concentration (Figure 2). Ethanol would vaporize rapidly from the microdroplets, thereby concentrating the reaction mixture, and we should be able to reduce the gelation time scale significantly in the aerosol experiment. Moreover, we are able to accelerate gelation by increasing temperature (Figure 3). We inferred from the bulk liquid experiments that we should be able to produce porous $Fe_xO_yC_z$ gel particles in an aerosol reactor with residence times of a few minutes by atomizing a solution which would nominally give a gel in the bulk experiment in an hour.

Matching Time Scales. Aerosol processes generally involve short time scales (milliseconds to seconds), while time scales of bulk sol−gel reaction processes are on the order of a few minutes to hours. The theme of this work is to merge these two time scales to obtain the batch chemistry in an aerosol experiment, by reducing the characteristic gelation time. The precursor solution in the atomizer is dilute enough so that formation of sol particles is very slow. However, as the solution is sprayed into micrometer-size droplets, evaporation of the volatile solvent (ethanol) causes the droplet to shrink rapidly, with a characteristic droplet shrinkage time of $\sim 5 \times 10^{-5}$ s. This rapid increase in the precursor concentration in the droplet leads to a faster sol−gel reaction as shown in Figure 2. This synthesis approach illustrated above is conceptually shown in Figure 5.

Analyses of Nanoparticles Obtained from Aerosol Experiment. To establish the qualitative similarity between the bulk and droplet experiments, energy-dispersive spectrometry (EDS) measurements were conducted on particles obtained from the bulk, and aerosol phase experiments. The extent of hydrolysis of $FeCl_3$ in the two cases was compared. Results show that the Fe:Cl ratio was reduced from 1:3 (in the precursor

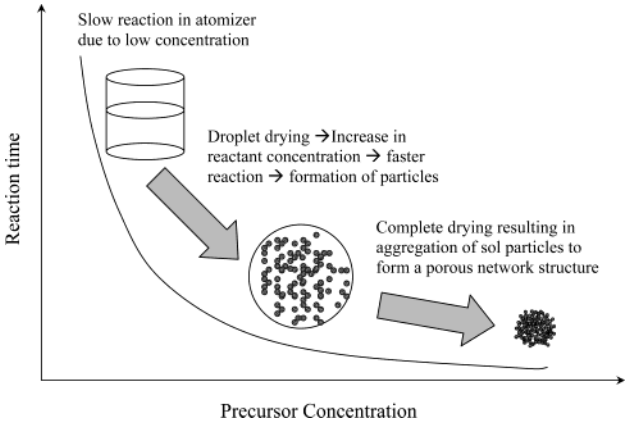

Figure 5. Conceptualization of the sol−gel reaction in the microdroplet to form porous particles.

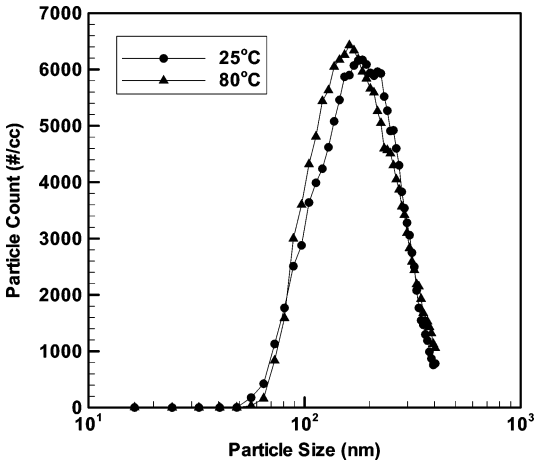

Figure 6. Product aerosol size distribution measured by DMPS.

solution) to 1:0.4 in the batch experiment, while it reduced to 1:0.8 in the aerosol experiment. Comparison of oxygen content would be an elegant way to compare the formation of iron oxide in two cases; however, quantitative estimation of low atomic weight elements (atomic numbers less than 10) cannot be accurately obtained.

Particle size distributions (PSD) using a differential mobility particle sizer (DMPS)[12] system are presented in Figure 6 and show a peak at about 180 nm, which shifts slightly to smaller particle sizes (160 nm) when the aerosol was heated to a higher temperature. The latter result is presumably due to faster evaporation of the solvent, which occurs while the gelation process is still continuing. A scanning electron microscope (SEM) image of the particles obtained in the aero-sol−gel experiment is shown in Figure 7 and indicates that the particles are spherical, are unagglomerated, and are of a size consistent with the DMPS measurements. SEM analysis was obtained with a JEOL-6500 FEG SEM at 5-kV operating voltage and a working distance of 4 mm.

An example of a TEM micrograph (Philips CM-30; accelerating voltage ∼300 kV) of these aero-sol−gel derived oxidizer particles is shown in Figure 8 and suggests the material does indeed have a porous structure. To quantify the porous nature of the particles, BET gas sorptometry measurements were conducted. On the basis of the PSD obtained, and assuming the particles to be dense solid material, the particles should have a

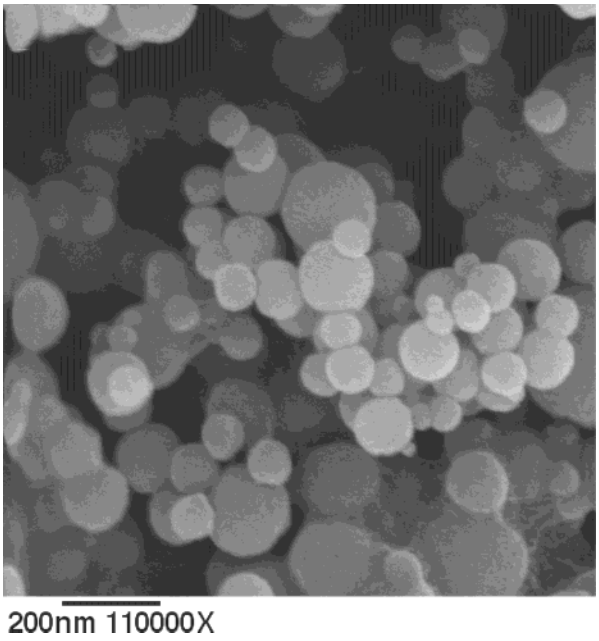

Figure 7. SEM image of particles obtained through the aerosol route.

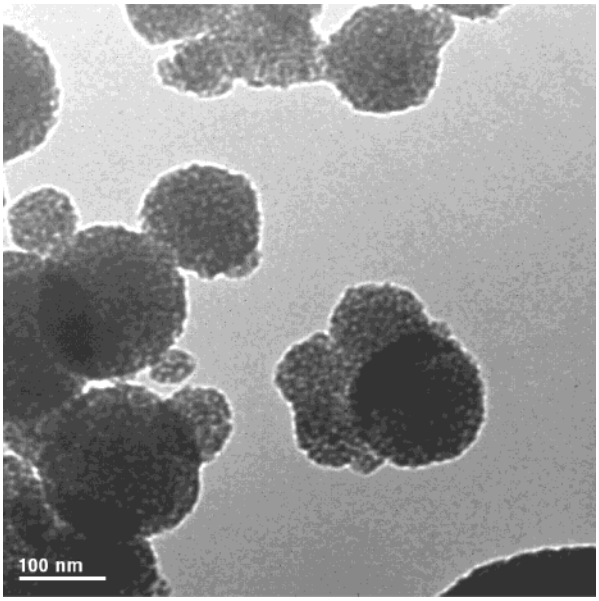

Figure 8. TEM image of the porous oxidizer particles obtained in the aerosol experiment.

Table 2. Variation of Surface Area of Particles with [Fe] in the Precursor Solution

[Fe]	measured particle size (electrical mobility diameter)	surface area (m^2/g)
0.1 M	180 nm	<3
0.2 M	180 nm	10
0.3 M	180 nm	210

surface area of ∼1 m^2/g. Furthermore, had the droplet shrunk to a nonporous dense particle, the resulting particle sizes would have been much smaller than the observed sizes. We summarize the results in Table 2 and show the measured particle size and specific surface area as a function of the precursor salt concentration. We first note that the particle size distribution does not depend on the precursor solution concentration! Since the characteristic evaporation time is very small (∼10^{-5} s), quick evaporation of solvent from the droplet surface

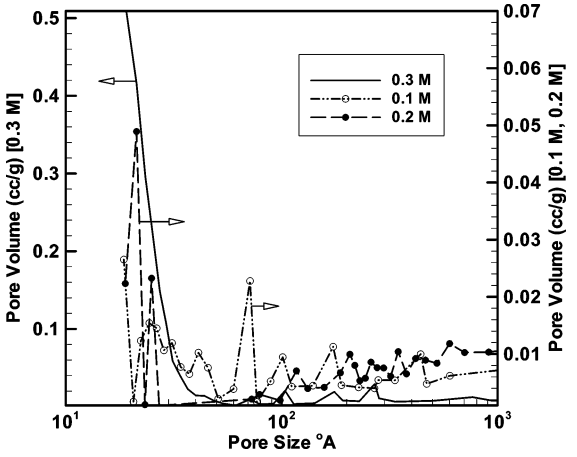

Figure 9. BJH adsorption pore volume distribution for a 0.1, 0.2, and 0.3 M [Fe] precursor solution.

increases the precursor concentration on the surface, and the mobility of molecules also reduces. Faster reaction at the surface causes the formation of a rigid gel on the surface, which does not allow further shrinkage of the particles. We have discussed the formation of a porous network of particles in a previous publication[12] by Kim et al. While the surface is solid-like, the interior of the particle is liquid-like, and it is the drying rate that determines the pore structure development. Another interesting result was the increase in surface area with increase in the concentration of the precursor solution. Surface area of as much as ~210 m^2/g was obtained when we increased the $FeCl_3$ concentration to 0.3 M in the precursor solution. The size of the particles of equivalent surface area is 5.3 nm assuming the density of iron oxide to be 5.4 g/cm^3, implying that the particle can be thought of as a spherical aggregate (fractal dimension = 3) composed of on average 5-nm primary particles. BJH adsorption pore volume distributions for different precursor solution concentrations are shown in Figure 9. We note that a very high pore volume is observed for the solution of higher concentration (left *y*-axis) while the pore volume is an order of magnitude smaller for the lower concentration (0.1 and 0.2 M) cases (right *y*-axis). A possible explanation for such a behavior could be that, in the high concentration (0.3 M) case, due to a high degree of supersaturation in the droplet, a large number of primary particles are formed which then link themselves in a network to form porous structure. In the higher concentration case, low supersaturation leads to nucleation of larger primary particles, leading to reduced surface area and pore volume. It is important to point out that such a test cannot be done for concentrations higher than 0.3 M because the solution becomes viscous and cannot be sprayed using a collision-type atomizer. The fact that we see no evidence of large pores (supported by TEM images) suggests that the particles are not hollow, which is very common for spray pyrolysis.[13−15] The particles are clearly porous with pore sizes on the order of ~2−3 nm. The sizes of these pores are close to the size of the estimated primary particle size.

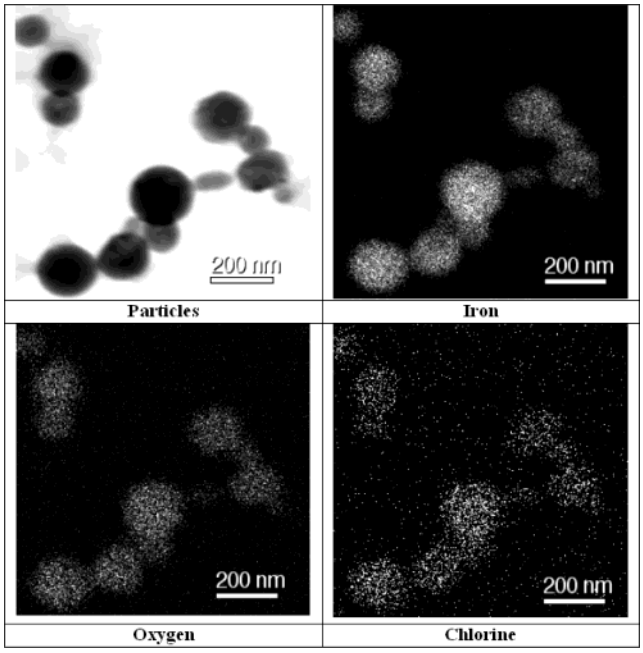

Figure 10. STEM elemental map showing the distribution of Fe, O, and Cl in the particles.

Assuming that all the iron in the precursor solution were converted to iron oxide and all the solvent evaporates, a 1-μm droplet (generated by the atomizer) would shrink to 92 nm. However, the DMPS measurements peak at about 180 nm. On the basis of this, we can compute a void fraction of about 90%, for a 0.1 M precursor case. In principle, with controlled evaporation, one should be able to lock the microstructure of the particles in a fairly wide size range, by controlling the vapor-phase pressure of the solvent and thus restricting the drying rate of droplets. Experiments are under way and the results shall be reported later.

Scanning transmission electron microscopy (STEM) elemental mapping on the particles have been obtained (Philips CM-30; accelerating voltage ~ 300 kV) to examine the hydrolysis of $FeCl_3$ and are shown in Figure 10. In an STEM map, the electrons scan the entire area of the image to identify the different elements present in the view. Clearly, iron and oxygen are uniformly distributed throughout the particles, suggesting the presence of iron oxide. A low intensity on the chlorine map suggests that there is some unreacted chlorine present.

Finally, to access the suitability of these materials as oxidizers, burn tests and in some cases ignition tests to measure the pressurization of an enclosed ignition were performed (at Los Alamos National Laboratories). A simple mixture of oxide-passivated nano-aluminum (primary particle sizes in 40-nm range) and aero-sol−gel derived iron oxide burned vigorously with a propagation speed of about 4 m/s. However, an ultrasonicated stoichiometric mixture (according to the thermite reaction in section I) generated by ultrasonicting the oxide/aluminum mixture (~25 wt % Al and 75 wt % Fe_2O_3 mixed intimately at nanoscale) in ethanol, followed by drying, resulted in a violent explosion as shown in the photograph in Figure 11. A pressure cell[16] test was performed on the aero-sol−gel iron oxide/aluminum nanoscale mixture wherein about 30 mg of the mixture

(13) Dubois, B.; Ruffier, D.; Odier, P. *J. Am. Ceram. Soc.* **1989**, *72*, 713.
(14) Gadalla, A. M.; Yu, H. F. *J. Mater. Res.* **1990**, *5*, 2923.
(15) Senzaki, Y.; Caruso, J.; Hampden-Smith, M. J.; Kodas, T. T.; Wang, M. L. *J. Am. Ceram. Soc.* **1995**, *78*, 2973.

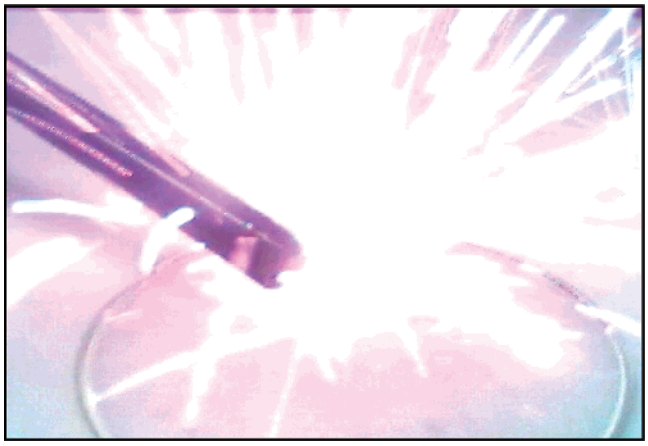

Figure 11. Photo of thermal ignition of iron oxide/aluminum nanoparticle mixture.

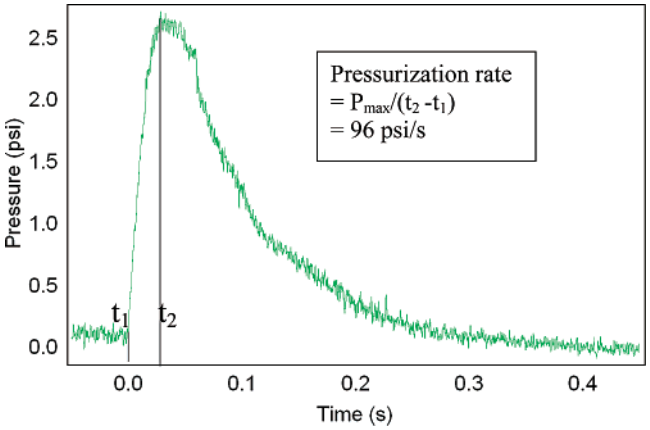

Figure 12. Pressure cell test on Fe_2O_3/Al nanocomposite.

was ignited in a small chamber of constant volume (13 cm^3) with a Nichrome wire, and the chamber pressure was monitored as a function of time. The observed pressurization rate of 96 psi/s presented in Figure 12 is less dynamic than the more traditional thermite reaction using Al/MoO_3 mixtures.[17] However, this difference is expected because Fe_2O_3 is known to be a slower oxidizer than MoO_3, and the Al/Fe_2O_3 (of density ~0.7 g/cm^3) mixture tested had a much higher density as compared to the Al/MoO_3 (of density ~0.1 g/cm^3) mixture and high-density materials are expected to have slower flame propagation. The presence of flaws in the low-density material allows convective burning while in a high-density material conductive burning is dominant, which is orders of magnitude slower.[17]

However, the nature of the sol−gel derived iron oxide is unique because of its highly porous nature and may afford the opportunity to infuse that material with organics, which would lead to much higher pressurization rates resulting from gas expansion. It is necessary to caution the reader that these nanothermite reactions of aluminum and metal oxides are extremely energetic. Reactions can be very explosive in the case of a few other oxidizers such as CuO and MoO_3; hence, it is advised that one should use very small quantities of such mixtures (less than 50 mg) while performing any ignition tests.

IV. Conclusions and Future Work

This paper reports on our efforts to employ sol−gel chemistry in the aerosol phase to prepare porous oxidizer particles composed of iron oxide that may have application to nanoenergetic compositions. We have shown the enhancement of bulk sol−gel reaction rate by increasing the concentration of reaction mixture in the droplet by controlled solvent evaporation. Characterization of these particles has shown that the material is identical to that obtained in the bulk experiments. These materials are shown to have a very high surface area enhancement when synthesized through the aerosol route. We have been able to obtain particles within a broad range of surface areas (3−210 m^2/g) by varying the amount of solvent present in the precursor solution. We believe that a nanocomposite, where we encapsulate Al nanoparticles in the aero-sol−gel oxidizer matrix, would react vigorously with much higher flame speeds and much faster energy release. The advantage of using sol−gel chemistry to obtain oxidizer particles is the possibility for infusing an organic material into the nanocomposite, which can cause gas expansion and further intensify the reaction.

Acknowledgment. We are grateful to Dr. Alexander E. Gash of the Lawrence Livermore Labs for his advice and insight into the sol−gel chemistry. We are also deeply indebted to Dr. Steve Son and Dr. James Busse of Los Alamos National Laboratories for doing the pressure cell measurements. This work was supported by the Army DURINT Center for Nano-Energetics Research.

CM034740T

(16) Son, S. F.; Asay, B. W.; Busse, J. R.; Jorgensen, B. S.; Bockmon, B.; Pantoya, M. *Proceedings of the International Pyrotechnics Society*, The Twenty-Eighth International Pyrotechnics Seminar, Adelaide, Australia, November 4−9, 2001.

(17) Son, S.; Busse, J.; Asay, B.; Bockmon, B.; Pantoya, M. *Proceedings of the International Pyrotechnics Society*, The Twenty-Ninth International Pyrotechnics Seminar, Colorado, July 14−19, 2002.